Encapsulation, visualization and expression of genes with biomimetically mineralized Zeolitc Imidazolate Framework – 8 (ZIF-8)

Arpita Poddar,[1,2] José J. Conesa,[3] Kang Liang,[4] Sudip Dhakal,[1] Philipp Reineck,[5] Gary Bryant,[6] Eva Pereiro,[3] Raffaele Ricco,[7] Heinz Amenitsch,[8] Christian Doonan,[9] Xavier Mulet,2 Cara M. Doherty,2 Paolo Falcaro,[7] and Ravi Shukla[1]*

1. Ian Potter NanoBiosensing Facility NanoBiotechnology Research Laboratory (NBRL), School of Science, RMIT University, Australia
2. CSIRO Manufacturing Clayton, Australia
3. ALBA Synchrotron Light Source MISTRAL Beamline – Experiments division, Spain
4. School of Chemical Engineering and Graduate School of Biomedical Engineering, University of New South Wales Australia
5. ARC Centre of Excellence for Nanoscale BioPhotonics, School of Science, RMIT University, Australia
6. Centre for Molecular and Nanoscale Physics, School of Science, RMIT University, Australia
7, Institute of Physical and Theoretical Chemistry, Graz University of Technology, Austria
8, Institute of Inorganic Chemistry, Graz University of Technology, Austria
9. Department of Chemistry and the Centre for Advanced Nanomaterials, The University of Adelaide, Australia

ABSTRACT. Recent work in biomolecule-metal–organic framework (MOF) composites have proven to be an effective strategy for the protection of proteins. However, for other biomacromolecules such as nucleic acids, the encapsulation into MOFs and the related characterizations are at is infancy. We herein report encapsulation of complete gene-set in zeolitic imidazolate framework-8 (ZIF-8) MOFs and intracellular expression of the gene delivered by the MOF composites. Using a GFP plasmid (plGFP) as a proof-of-concept genetic macromolecule, we show successful transfection of mammalian cells with plGFP for up to 4 days, demonstrating the feasibility of DNA@MOF biocomposites as intracellular gene delivery vehicles which occurs over relatively prolonged time points where the cargo nucleic acid is released gradually in order to maintain sustained expression.

KEYWORDS: ZIF-8, MOFs, gene therapy, transfection, DNA, encapsulation, functional activity.

Gene therapy holds great promise in disease treatment; however, the delivery of therapeutic genes is a severe impediment in the overall success of this approach[1-3]. The efficacy of gene therapy has been greatly affected by the inadequacy of delivery vectors. Over 70% of the gene therapy clinical trials involve viral vectors and only about 11% of trials utilize non-viral delivery systems[4-5]. Viral therapy has been most effective for monogenic diseases like severe combined immune deficiency (ADA-SCID), in which disease pathogenesis is attributed to a single gene[6]. However, diseases like cancer are multifactorial polygenic diseases and therapeutic-loaded vectors are yet to complete Phase III trials or any large statistically powered Phase II trials[7]. Although conventional viral systems like adenoviral and lentiviral systems are powerful vectors with high transfection efficacy, their application in the clinical setting raises significant concerns of cytotoxicity, pathogenicity, non-targeted insertions, DNA carrying capacity, potential side effects due to small sample size of cases studied and short follow up periods[8-9]. Non-viral delivery systems are safer and less immunogenic, are relatively inexpensive to produce and have a large DNA carrying capacity while allowing for easy modifications to the system[10]. However, these carriers have several limitations that restrict the practical applications for the delivery of therapeutics[11]. Currently, the only non-viral delivery vehicles that are in clinical trial are lipid based nano and micro systems[12]. However, they can be unreliable for intravenous delivery as their structure can be hampered in the presence of serum; as a result, large aggregates are be formed[7, 13]. For example, one of the most commonly studied pH responsive polymers is poly(2-(N,N-dimethylamino)ethyl methacrylate) (pDMAEMA). But the polymer molecular weight, composition with DNA, synthesis methods and aggregation and haemagglutination in the presence of serum proteins and blood cells has resulted in numerous contradictory results[14]. Other important cationic lipids like poly(l-lysine) (PLL), one of the most often used polymers for the complexing and delivery of DNA, has been known to be cytotoxic and possess low capacities for maintaining DNA integrity and endosomal escape[9]. Due to such conflicting reports, up to 2017, only 0.24% of all the reported studies on gene therapy have been reported to investigate non-viral delivery systems[15]. The limitations arise from the inability and significant challenges in the capacity of the non-viral vectors to maintain the chemical and physical integrity of DNA, successful entry through the cell membrane,

endosomal escape prior to nuclear uptake for expression of the gene through transcription and translation[16]. Therefore, development of improved synthetic systems that allows the vector to address the above limitations is essential. In this study, we report the potential of self-assembled porous systems of metal-organic frameworks (MOFs) in their ability to function as suitable gene therapy systems for DNA delivery.

MOFs are a family of porous materials with well-defined coordination geometry comprising of metal ions linked to organic bridging ligands[17]. Owing to their high loading capacity, controlled release profiles, biodegradability, and versatile functionality, nanoscale MOFs serve as ideal platforms for biological applications[18-24]. A particular attraction of MOFs is their ability to bio-conjugate, infiltrate and encapsulate biomolecules; thus MOF biocomposites can be prepared with controlled stability, release and biological functions[25-27]. Zeolitic imidazolate frameworks (ZIFs) are members of the MOF family and are made of zinc ions coordinated by imidazole rings to form topological isomorphs of zeolites. They have demonstrated biocompatibility, biodegradability, protection and potential applications in antitumor therapy, protection of biomarkers and encapsulation of therapeutics[28-29]. Several MOFs, including ZIFs have been used to successfully deliver siRNAs and oligonucleotides and encapsulation of proteins and cells have also been reported[30-34]. However, when these approaches were used for either the biocojugation or loading of DNA, only short nucleotide sequences were used. Specifically, the largest nucleic acids that have been incorporated do not exceed 50 base-pairs[35-38], which do not encompass functional genes suitable for gene delivery[39]. The short size range is severely limited to applications with DNA oligonucleotides and RNA interference employing siRNAs and miRNAs[40]. Unlike siRNAs/miRNAs which are 20-25 nucleotides and functionally active, DNA oligonucleotides of short sequences do not possess functional activity within cells. Hence, the reported studies using oligonucleotides have been limited to score the real potential of MOFs as gene delivery vehicles which retain structural and functional activity of the cargo nucleic acid for gene therapy. In this study, we investigate MOFs like ZIF-8 polymorphs, made of zinc nodes connected by 2-methylimidazole (2mIM), as delivery systems for gene therapy by demonstrating the encapsulation of an entire plasmid DNA (6.5 kilo base-pairs) molecule.

A plasmid represents a DNA molecule that harbors intact genes on their sequences. Plasmids are circular, double-stranded DNA (dsDNA) sequences most commonly found in bacteria that can also be expressed in mammalian cells following transfection[41-42]. A plasmid expressing green fluorescent protein (plGFP) was selected as the representative plasmid for proof-of-concept study as they are extensively characterized, easily available and routinely used for cellular and molecular biology studies[43-44]. They carry genes that code for a green fluorescent protein (GFP). The plGFP itself is non-fluorescent, but when transcribed and translated within cellular machinery, express a non-toxic protein, GFP, which emits a strong green fluorescence under UV light.

For the synthesis of DNA encapsulated ZIF-8 (DNA@ZIF-8), the process of biomimetic mineralization was followed according to the protocol published by Liang et al.[45], where the presence of the biomolecule triggers in the formation of $Zn(2mIM)_2$. The effect of the plGFP as biomimetic mineralization agent was tested using Small-Angle X-ray Scattering at Elettra synchrotron; using a stop-flow set-up the rapid formation of $Zn(2mIM)_2$ particles in presence of DNA was confirmed (see Supporting XX). The obtained MOF bio-composites were termed plGFP@ZIF-8. Encapsulation of DNA within ZIF-8 was visualized using a readily available DNA dye, propidium iodide (PI). PI is a fluorescent DNA stain commonly used in laboratories for staining cellular DNA[46-48]. In the presence of exposed DNA, it intercalates between the DNA bases with little or no sequence preference and fluorescence is enhanced 20- to 30-fold, the fluorescence excitation maximum is shifted ~30–40 nm to the red and the fluorescence emission maximum is shifted ~15 nm to the blue. On treatment of plGFP@ZIF-8 with PI, no fluorescence signal was detected to denote the presence of DNA. Chelators like ethylenediaminetetraacetic acid (EDTA) are known to dissolve ZIF-8 [45], and plGFP@ZIF-8 when treated with EDTA dissolved the ZIF-8, and a strong fluorescent signal from plGFP was then observed. The straightforward staining procedure indicates that in intact plGFP@ZIF-8, DNA was successfully shielded from the access of PI by ZIF-8 framework. To verify structural and functional integrity of DNA within the biocomposites system, plGFP released from the MOF biocomposites were transfected into mammalian cell line. Green fluorescence, i.e., GFP can be detected in the cells within 24 hours of transfection similar to transfection with control plGFP that were

not part of MOF biocomposites. The encapsulation and release mechanism of plGFP@ZIF-8 thus does not disrupt the functional activity of the plasmid because expression of protein occurs due to lack of significant damage to the plasmid structure. In order to check for cellular uptake of plGFP@ZIF-8, the MOF biocomposites were then transfected without prior release into the mammalian cells and treatment was carried out for 3.5 hours. Cellular internalization of plGFP@ZIF-8 particles were visualized at 24 hours using correlative cryo-epifluorescence microscopy and soft X-ray cryo tomography (cryo-SXT), the only modality that allows imaging of whole cell samples in its native state without any chemical treatment or sectioning[49-50]. For expression of protein from plGFP@ZIF-8 system, green fluorescence in the cells could be recorded at 96 hours post treatment, indicating a gradual expression rather than

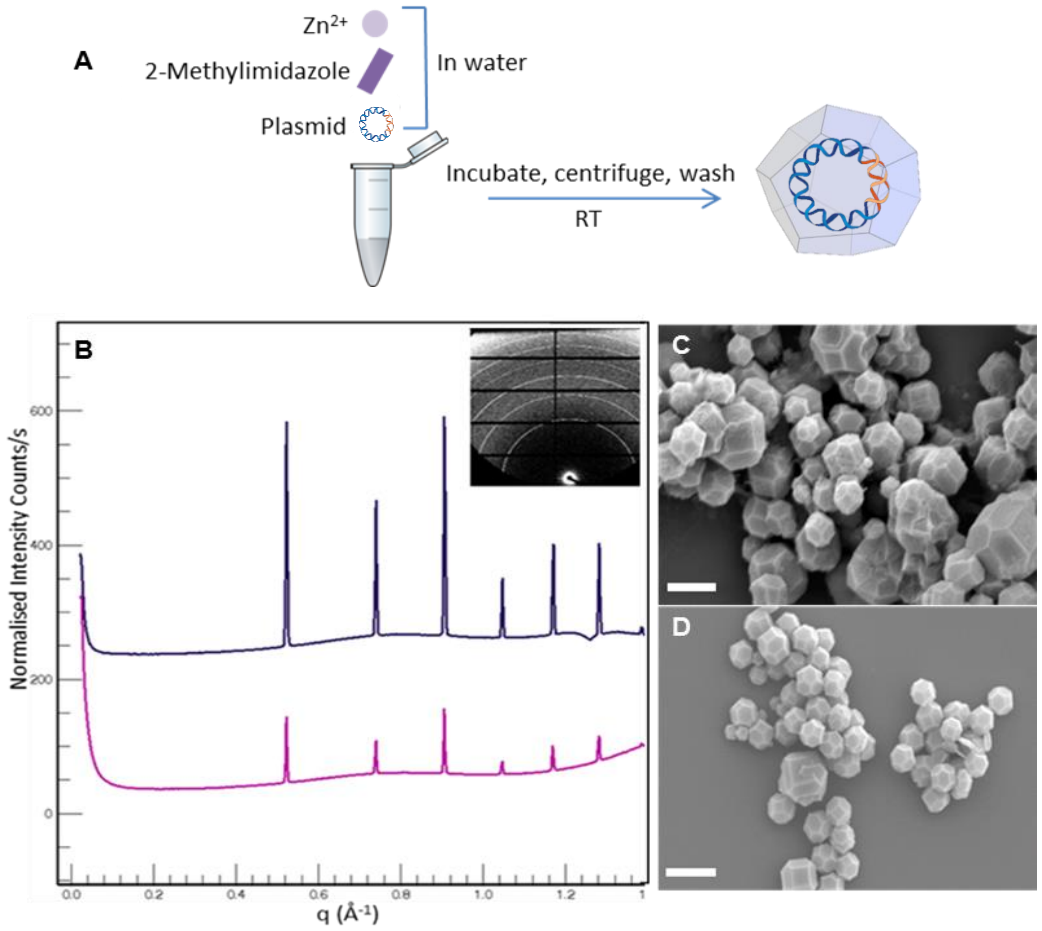

immediate release and expression from the MOF biocomposites.

Figure 1. Schematic of synthesis of plasmid plGFP @ ZIF-8 based on biomimetic mineralization (A); Small-Angle X-ray Scattering (SAXS) patterns of pure ZIF-8 (black) and biomimetically mineralised plGFP@ ZIF-8 (purple). Inset: 2D representation of SAXS patterns of the composite materials (B); Scanning electron microscopy image of pure ZIF-8 (C) and plGFP@ZIF-8 (D), scale bars 1 μm.

In a typical experiment, DNA (0.34 pM plGFP) was added to aqueous solutions of 2mIM (160 mM) followed by zinc acetate (40 mM) at room temperatures (**Figure 1A**). The clear solution became cloudy and turbid within 10-15 seconds, and following incubation of 10 or 120 minutes, the solution was centrifuged at 10,000 rcf for 10 minutes. The supernatant was kept aside for further analysis and the pellet was washed with ethanol to recover the plGFP plasmid-loaded ZIF-8 particles. Small angle X-ray scattering (SAXS) studies on the recovered pellet indicated identical crystalline phases between the pellet particles and conventionally synthesized ZIF-8 MOFs with matching indices (Figure 1B). Scanning electron microscopy (SEM) studies showed that the plGFP@ZIF-8 had similar morphology to conventionally synthesized pure ZIF-8 (**Figure 1C, D**).

Centrifuging pure DNA dissolved in water at 10,000 rcf does not form a pellet or precipitate DNA. To confirm that the DNA did not stay in the supernatant during plGFP@ZIF-8 synthesis, both the supernatant and the EDTA treated pellet were run on a 1% agarose gel electrophoresis (Figure 2A). A distinct band was visible in the pellet lane which is similar in intensity to the control naked DNA. However, only a very

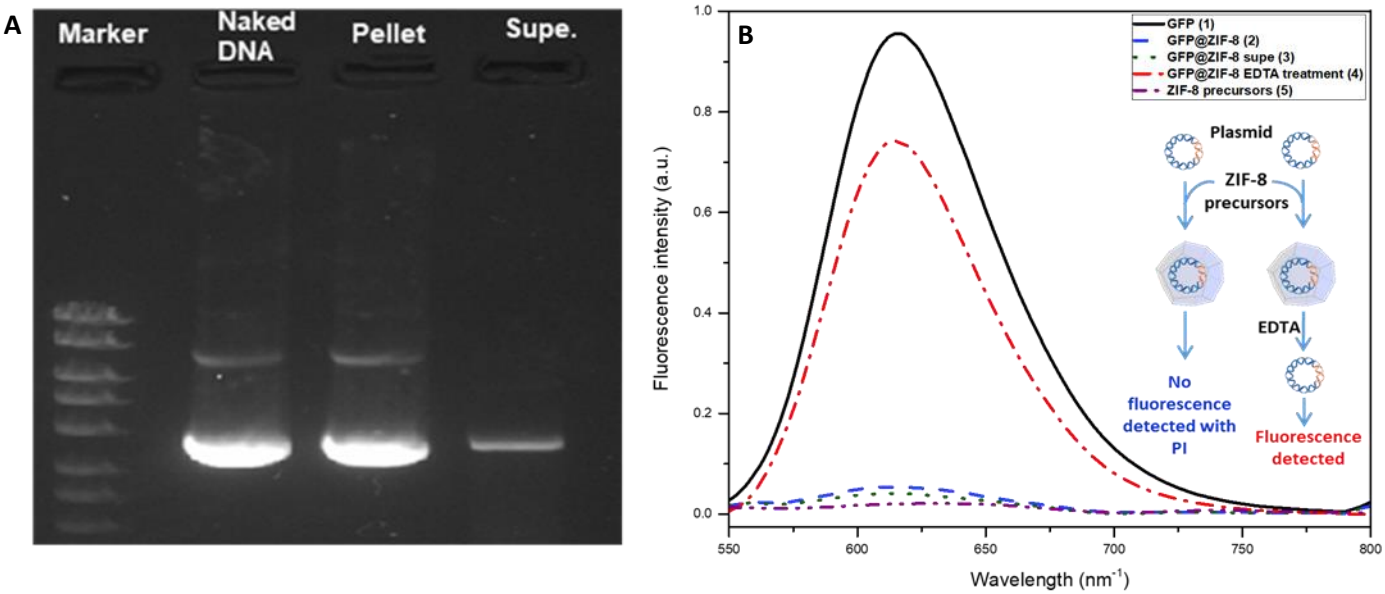

Figure 2. Agarose gel electrophoresis of plGFP@ZIF-8. Left-right: DNA Hyperladder 1, naked DNA (0.34 pM), post synthesis pellet, supernatant (A). Fluorescence emission spectra of DNA – Labeling with PI - plGFP (1), plGFP@ZIF-8 (2), plGFP@ZIF-8 synthesis solution supernatant (3), plGFP@ZIF-8 with EDTA treatment (4) and ZIF-8 precursors without DNA (5) (B).

faint band could be seen in case of the supernatant. This demonstrates that only a minor amount of DNA

(9%) is present in the supernatant and almost 90% DNA quantity is present with the MOF crystals in the pellet.

PI was employed to further assess the encapsulation of the plasmid DNA. Following synthesis, the pellet was treated with 1 μg ml^{-1} PI. Pure DNA on treatment with PI gives a peak at 617 nm which is the emission maxima of PI bound DNA (**Figure 2B**, black). This peak is absent in PI treated plGFP@ZIF-8 (pellet, blue) as well as supernatant (green). However, when the MOF particles are dissolved by using EDTA (20 mM), the fluorescence signal peak can be easily detected (as shown by the red curve in Figure 2). This indicates that DNA was encapsulated inside ZIF-8; when PI is added to it, the dye is unable to access or bind DNA as it would have if the DNA had been surface conjugated and leads to the absence of emission maxima of PI-DNA in the pellet. On addition of EDTA to the pellet, the ZIF-8 dissolves due to chelation of the zinc ions by EDTA[30], and DNA is released which is then free to interact and bind with the dye, showing fluorescence spectra with peak at 617nm.

In order to prove the encapsulated plasmid DNA remains functionally intact, transfection assays were carried out with the released plasmids. Human epithelial cells from prostate cancer (PC-3) were transfected with pure plGFP plasmids and plGFP@ZIF-8 with 10 and 120 minutes of incubation with precursors during synthesis. The cells were fixed and stained with Hoechst 3342 dye 24 hours post transfection and imaged on a confocal laser scanning microscope (CLSM) (**Figure 3**). Fluorescence from is present only when the plasmid has been transcribed and translated to express the green fluorescent protein inside the cells. Any significant damage to the plasmid structure will not allow the protein to be efficiently expressed and consequently, the cells will not show fluorescence. Untreated cells do not show any green fluorescence (**Figure 3A**). However, cells transfected with pure plGFP (**Figure 3B**), plGFP released from ZIF-8 with 120 (**Figure 3C**) and 10 (**Figure 3D**) minutes of incubation during synthesis showed fluorescence. This indicates that the DNA does not undergo substantial damage during the encapsulation process that can negatively impact its functional activity and thus, remains functionally intact.

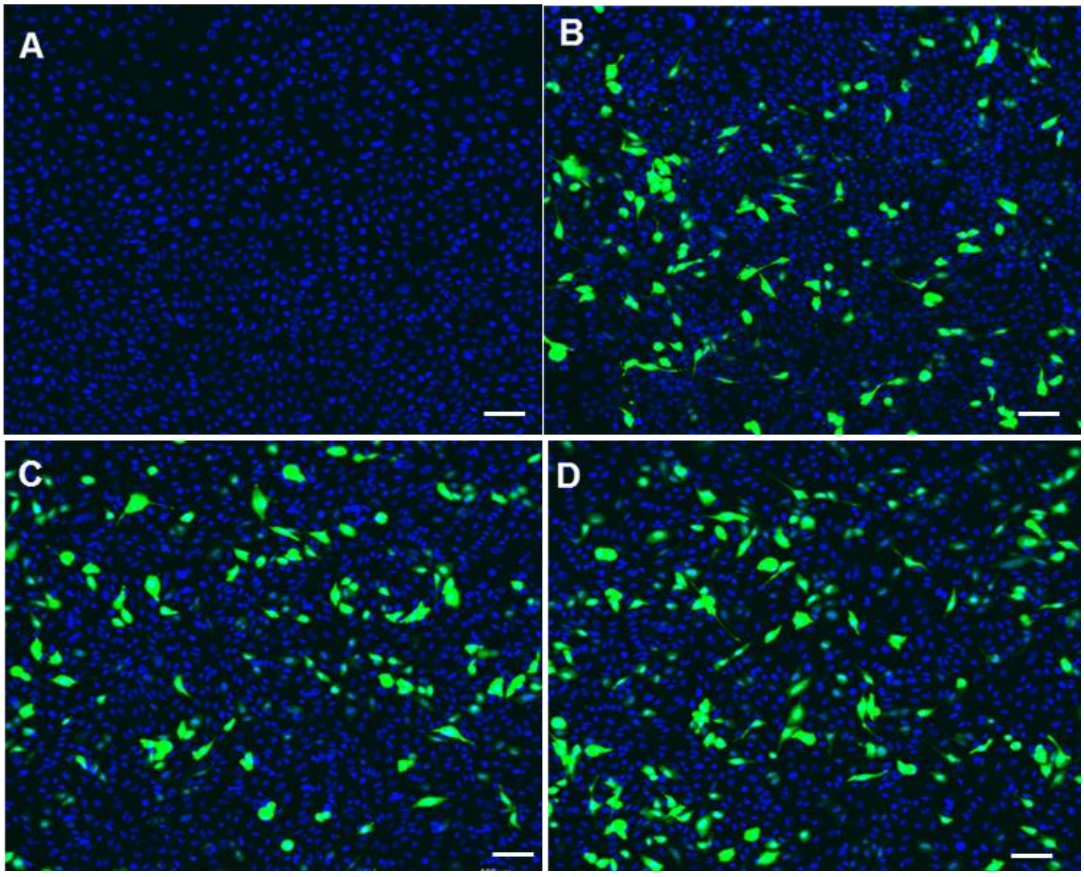

Figure 3. DNA remains functionally intact – Untreated PC-3 cells (A), Cells transfected with plGFP (B), Cells transfected with plGFP previously encapsulated in ZIF-8 synthesized with 120 (C) and 10 (D) minute incubation periods. All transfections allowed to occur for 24 hours with a concentration of 500 ng DNA. Blue – cell population as seen by Hoechst 33342 nuclear stain. Green – fluorescence due to protein expression from plGFP, scale bar 100µm.

For evaluating the gene delivery capacity of plGFP@ZIF-8 and their impact on cellular viability, transfection assays and MTT viability assays were carried out with pure and biomimetically mineralized ZIF-8 washed in water and exposed to PC-3 cells for a period of 3.5 hours. Following which treatment media was replaced and transfection and viability results were recorded (**Figure 4A-D**). The plGFP@ZIF-8 transfected cells were fixed and stained with nuclear stain Hoechst 33342 dye at 24, 48, 72 and 96 hours post transfection and imaged on a CLSM. A further control treatment involved co-transfection with pure ZIF-8 and plGFP. No green fluorescence is detected from either untreated cells (**Figure 4A**) or ZIF-8 and plGFP co-transfected cells (**Figure 4B**), however, green fluorescence from plGFP@ZIF-8 treated cells start becoming significant from the 96 hour time point (**Figure 4C**), prior to which no significant fluorescence signal could be detected. It is clear that cellular transfection with DNA@ZIF-8 occurs over

a prolonged time as compared to regular transfection. This could possibly be due to endosome mediated uptake or macropinocytosis where ZIF-8 is gradually broken down in the acidic environment within the cell to cause sufficient degradation for release of plasmid. As the gene expression becomes pronounced gradually over time by 96 hours, the DNA is not instantaneously exposed to the cellular machinery on delivery. It is postulated that although ZIF-8 starts releasing around 50% DNA by 72 hours (**Figure S4**), parts of dispersing ZIF-8 might remain associated with the plasmid~~, presumably by hydrogen bonds,~~ and dissociate slowly (**Figure 4G**). The regulatory portion of the plasmid on the DNA sequence are the promoter regions. Promoter sequences are responsible for activating the enzyme RNA polymerase and several transcription factors, which in turn are responsible for transcribing the coding DNA sequence into an mRNA sequence[51]. Further downstream processing results in the translation of mRNA into proteins, leading to successful expression of the genetic element. The RNA polymerase enzyme forms a large multiprotein complex of more than 500 kDA around the DNA fragment at the start of transcription. If transcription has been activated, the enzyme machinery is capable of knocking off or dislodging remaining ZIF-8 fragments on the DNA and hastening ZIF-8 degradation. However, if the ZIF-8 fragments mask the promoter or transcription start sites, the polymerase complex is unable to access DNA to activate transcription and expression is achieved only when ZIF-8 is completely removed from the DNA.

plGFP@ZIF-8 also did not show any long-term cellular toxicity up to 96 hours. Effect on cellular toxicity was determined using MTT assays in which 82% and 96% viabilities were obtained for DNA@ZIF-8 transfected cells at 24 and 96 hours respectively (**Figure 4D**). The internalization of plGFP@ZIF-8 in PC-3 cells was further studied using correlative cryo-epifluorescence microscopy and cryo-SXT, the only imaging modality that allows imaging of 3D maps of vitrified whole-cell samples in its native state, thus circumventing chemical treatment or sectioning. The use of soft X-rays (with wavelengths in the range of the water window, i.e., 2.3–4.4 nm), provides the possibility to obtain high contrast images from unstained biological samples[52]. We were thus able to visualize the presence of plGFP@ZIF-8 at 24 hours within cytoplasm and endocytic organelles of PC-3 cells in physiological conditions with minimal radiation damage (**Figure 4E-F**).

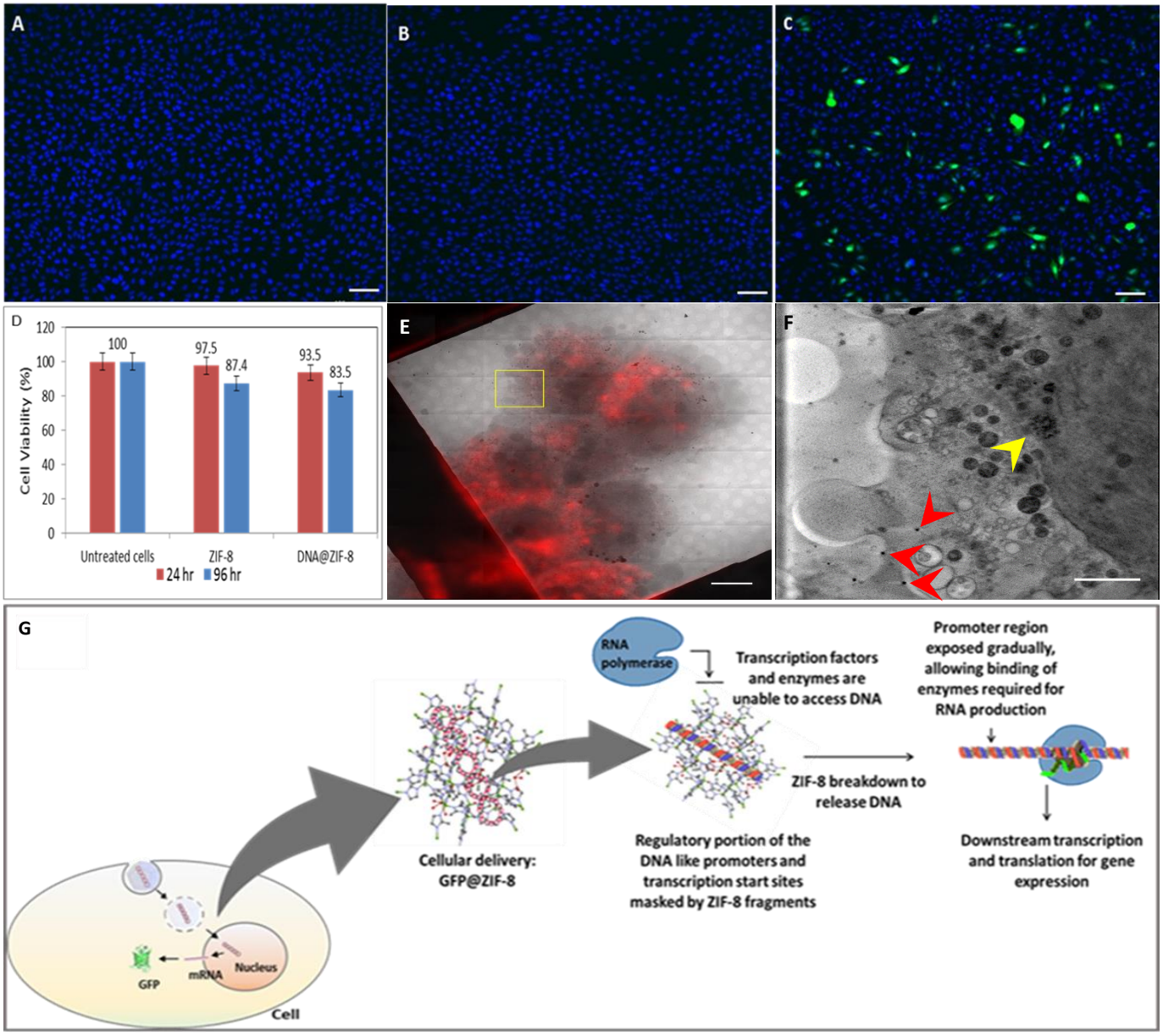

Figure 4. Delivery potential, effect on viability and intracellular detection; PC-3 incubated with plGFP@ZIF-8 for 3.5 hours – Untreated PC-3 cells (A), pure ZIF-8 and plGFP co-transfected PC-3 (B) and plGFP@ZIF-8 transfected PC-3 (C) cells at 96 hours; cellular viability of PC-3 cells in the presence of plGFP@ZIF-8 and pure ZIF-8 (D) at 24 and 96 hours. All transfections carried out with a concentration of 500 ng DNA, Blue – cell population as seen by Hoechst 33342 nuclear stain. Green – fluorescence due to protein expression from plGFP, scale bar 100 µm. Overlay image of cryo-epifluorescence acidic organelles signal (red) and cryo-Soft X-ray projection images mosaic (E). The area squared in yellow corresponds to the tomogram section shown in (F). Cryo-SXT three-dimensional tomogram section through XY plane, the yellow arrow head points to an endocytic organelle containing densities compatible with ZIF-8 MOFs and the red arrow heads point to high intracytoplasmic densities compatible with ZIF-8 MOFs (F). Scale bars: 10 µm (E), 2 µm (F). Schematic of proposed gene expression mechanism on cellular delivery of plGFP@ZIF-8. Gene expression is visualized as green fluorescence produced in the cells (G).

In conclusion, we demonstrate a rapid and efficient method to utilize MOFs for carrying large size intact gene sets like plasmid vectors; the encapsulated plasmid retains its functional activity while displaying intracellular delivery potential. Visualizing encapsulation by MOFs using PI staining is easy to use, and cost-effective as compared to other techniques of qualitative polymerase chain reaction (qPCR) amplifications and transmission electron microscopy (TEM) imaging; overcoming shortcomings like lengthy sample preparation where DNA elements need to be labeled with heavy atoms prior to encapsulation (TEM) and size limitations and optimization sensitivities of qPCR assays[53]. Furthermore, in the field of gene therapy, a major concern for current non-viral vectors like plasmids is that the delivery method can often lead to reduced efficient expression due to damage of plasmid DNA backbones. Thus, the genetic expression of plGFP shown in this study utilizing ZIF-8-based MOFs as delivery systems demonstrates the ability of MOFs to maintain the chemical and physical integrity of DNA by conserving its function. The retention of functional activity, intracellular delivery and expression of encapsulated gene occurs over relatively prolonged time periods without cytotoxicity. This has huge potential in the field of gene therapy where delivery system itself should be non-toxic and in cases where a sustained expression over time is required instead of burst release of therapeutic load. The utilization of water washed plGFP@ZIF-8 for cellular expression and gene delivery could also have an impact on the uptake and efficiency. It is postulated that separate polymorphs of plGFP@ZIF-8 can result on washing with water in place of ethanol, and tailoring of synthesis conditions to deliver the therapeutic gene in accordance to the requirements of individual cases forms the basis of our future studies. It is expected that this approach will result in a controlled gene delivery agent that protects and maintains functional activity of DNA and affords customized expression of genes leading to specifically designed persistence of therapeutic levels *in vivo*.

References

1. Yin, H.; Kanasty, R. L.; Eltoukhy, A. A.; Vegas, A. J.; Dorkin, J. R.; Anderson, D. G., Non-viral vectors for gene-based therapy. *Nature Reviews Genetics* **2014,** *15*, 541.
2. Net, G. T. Diseases Treated by Gene Therapy. http://www.genetherapynet.com/JoomlaTest2/index.php?option=com_content&view=article&id=164:diseases-treated-with-gene-therapy-&catid=97:patient-information&Itemid=14 (accessed May 23, 2018).

3. Hudecek, M.; Izsvak, Z.; Johnen, S.; Renner, M.; Thumann, G.; Ivics, Z., Going non-viral: the Sleeping Beauty transposon system breaks on through to the clinical side. *Critical reviews in biochemistry and molecular biology* **2017**, 1-26.
4. Gonçalves, G. A. R.; Paiva, R. d. M. A., Gene therapy: advances, challenges and perspectives. *Einstein* **2017,** *15* (3), 369-375.
5. Ginn, S. L.; Amaya, A. K.; Alexander, I. E.; Edelstein, M.; Abedi, M. R., Gene therapy clinical trials worldwide to 2017: An update. *The Journal of Gene Medicine* **2018,** *20* (5), e3015.
6. Kay, M. A., State-of-the-art gene-based therapies: the road ahead. *Nature Reviews Genetics* **2011,** *12*, 316.
7. Das, S. K.; Menezes, M. E.; Bhatia, S.; Wang, X.-Y.; Emdad, L.; Sarkar, D.; Fisher, P. B., Gene Therapies for Cancer: Strategies, Challenges and Successes. *Journal of cellular physiology* **2015,** *230* (2), 259-271.
8. Yang, N., An overview of viral and nonviral delivery systems for microRNA. *International Journal of Pharmaceutical Investigation* **2015,** *5* (4), 179-181.
9. Marguillier, L.; Dubruel, P.; Van Vlierberghe, S., Gene Therapy Approaches Toward Biomedical Breakthroughs. In *Polymer and Photonic Materials Towards Biomedical Breakthroughs*, Van Hoorick, J.; Ottevaere, H.; Thienpont, H.; Dubruel, P.; Van Vlierberghe, S., Eds. Springer International Publishing: Cham, 2018; pp 153-176.
10. Chira, S.; Jackson, C. S.; Oprea, I.; Ozturk, F.; Pepper, M. S.; Diaconu, I.; Braicu, C.; Raduly, L.-Z.; Calin, G. A.; Berindan-Neagoe, I., Progresses towards safe and efficient gene therapy vectors. *Oncotarget* **2015,** *6* (31), 30675-30703.
11. A, A., Gene Delivery. In *Manufacturing of Gene Therapeutics*, Subramanian, G., Ed. Springer, Boston, MA: 2002; pp 245-272.
12. Ginn Samantha, L.; Amaya Anais, K.; Alexander Ian, E.; Edelstein, M.; Abedi Mohammad, R., Gene therapy clinical trials worldwide to 2017: An update. *The Journal of Gene Medicine* **2018,** *20* (5), e3015.
13. Dash, P. R.; Read, M. L.; Barrett, L. B.; Wolfert, M. A.; Seymour, L. W., Factors affecting blood clearance and in vivo distribution of polyelectrolyte complexes for gene delivery. *Gene Ther* **1999,** *6* (4), 643-50.
14. Dubruel, P.; Schacht, E., Vinyl Polymers as Non-Viral Gene Delivery Carriers: Current Status and Prospects. *Macromolecular Bioscience* **2006,** *6* (10), 789-810.
15. Hidai, C.; Kitano, H., Nonviral Gene Therapy for Cancer: A Review. *Diseases* **2018,** *6* (3), 57.
16. Wiethoff, C. M.; Middaugh, C. R., Barriers to Nonviral Gene Delivery. *Journal of Pharmaceutical Sciences* **2003,** *92* (2), 203-217.
17. Zhou, H. C.; Long, J. R.; Yaghi, O. M., Introduction to metal-organic frameworks. *Chem Rev* **2012,** *112* (2), 673-4.
18. Horcajada, P.; Gref, R.; Baati, T.; Allan, P. K.; Maurin, G.; Couvreur, P.; Ferey, G.; Morris, R. E.; Serre, C., Metal-organic frameworks in biomedicine. *Chem Rev* **2012,** *112* (2), 1232-68.
19. Wuttke, S.; Braig, S.; Prei; Zimpel, A.; Sicklinger, J.; Bellomo, C.; Radler, J. O.; Vollmar, A. M.; Bein, T., MOF nanoparticles coated by lipid bilayers and their uptake by cancer cells. *Chem. Commun.* **2015,** *51* (87), 15752-15755.
20. Doonan, C.; Ricco, R.; Liang, K.; Bradshaw, D.; Falcaro, P., Metal-Organic Frameworks at the Biointerface: Synthetic Strategies and Applications. *Acc Chem Res* **2017,** *50* (6), 1423-1432.
21. Illes, B.; Wuttke, S.; Engelke, H., Liposome-Coated Iron Fumarate Metal-Organic Framework Nanoparticles for Combination Therapy. *Nanomaterials* **2017,** *7* (11), 351.
22. Horcajada, P.; Chalati, T.; Serre, C.; Gillet, B.; Sebrie, C.; Baati, T.; Eubank, J. F.; Heurtaux, D.; Clayette, P.; Kreuz, C.; Chang, J.-S.; Hwang, Y. K.; Marsaud, V.; Bories, P.-N.; Cynober, L.; Gil, S.; Ferey, G.; Couvreur, P.; Gref, R., Porous metal-organic-framework nanoscale carriers as a potential platform for drug delivery and imaging. *Nature materials* **2010,** *9* (2), 172-178.
23. Chen, W.; Wu, C., Synthesis, functionalization, and applications of metal-organic frameworks in biomedicine. *Dalton transactions (Cambridge, England : 2003)* **2018,** *47* (7), 2114-2133.

24. Li, S.; Wang, K.; Shi, Y.; Cui, Y.; Chen, B.; He, B.; Dai, W.; Zhang, H.; Wang, X.; Zhong, C.; Wu, H.; Yang, Q.; Zhang, Q., Novel Biological Functions of ZIF-NP as a Delivery Vehicle: High Pulmonary Accumulation, Favorable Biocompatibility, and Improved Therapeutic Outcome. *Adv. Funct. Mater.* **2016,** *26* (16), 2715-2727.
25. Li, S.; Huo, F., Metal-organic framework composites: from fundamentals to applications. *Nanoscale* **2015,** *7* (17), 7482-7501.
26. Kuppler, R. J.; Timmons, D. J.; Fang, Q.-R.; Li, J.-R.; Makal, T. A.; Young, M. D.; Yuan, D.; Zhao, D.; Zhuang, W.; Zhou, H.-C., Potential applications of metal-organic frameworks. *Coord. Chem. Rev.* **2009,** *253* (23–24), 3042-3066.
27. McKinlay, A. C.; Morris, R. E.; Horcajada, P.; Ferey, G.; Gref, R.; Couvreur, P.; Serre, C., BioMOFs: metal-organic frameworks for biological and medical applications. *Angew Chem Int Ed Engl* **2010,** *49* (36), 6260-6.
28. Wu, Q.; Niu, M.; Chen, X.; Tan, L.; Fu, C.; Ren, X.; Ren, J.; Li, L.; Xu, K.; Zhong, H.; Meng, X., Biocompatible and biodegradable zeolitic imidazolate framework/polydopamine nanocarriers for dual stimulus triggered tumor thermo-chemotherapy. *Biomaterials* **2018,** *162*, 132-143.
29. Liang, W.; Ricco, R.; Maddigan, N. K.; Dickinson, R. P.; Xu, H.; Li, Q.; Sumby, C. J.; Bell, S. G.; Falcaro, P.; Doonan, C. J., Control of Structure Topology and Spatial Distribution of Biomacromolecules in Protein@ZIF-8 Biocomposites. *Chem. Mater.* **2018,** *30* (3), 1069-1077.
30. Liang, K.; Ricco, R.; Doherty, C. M.; Styles, M. J.; Bell, S.; Kirby, N.; Mudie, S.; Haylock, D.; Hill, A. J.; Doonan, C. J.; Falcaro, P., Biomimetic mineralization of metal-organic frameworks as protective coatings for biomacromolecules. *Nat Commun* **2015,** *6*, 7240.
31. Liang, K.; Coghlan, C. J.; Bell, S. G.; Doonan, C.; Falcaro, P., Enzyme encapsulation in zeolitic imidazolate frameworks: A comparison between controlled co-precipitation and biomimetic mineralisation. *Chem. Commun.* **2015,** *52* (3), 473-476.
32. Liang, K.; Carbonell, C.; Styles, M. J.; Ricco, R.; Cui, J.; Richardson, J. J.; Maspoch, D.; Caruso, F.; Falcaro, P., Biomimetic Replication of Microscopic Metal-Organic Framework Patterns Using Printed Protein Patterns. *Adv Mater* **2015,** *27* (45), 7293-8.
33. Caruso, F.; Cui, J.; Richardson, J., Metal-Organic Framework Coatings as Cytoprotective Exoskeletons for Living Cells. **2016,** *28* (ADVANCED MATERIALS), 7910 - 7914 (5).
34. He, C.; Lu, K.; Liu, D.; Lin, W., Nanoscale metal-organic frameworks for the co-delivery of cisplatin and pooled siRNAs to enhance therapeutic efficacy in drug-resistant ovarian cancer cells. *Journal of the American Chemical Society* **2014,** *136* (14), 5181-4.
35. Peng, S.; Bie, B.; Sun, Y.; Liu, M.; Cong, H.; Zhou, W.; Xia, Y.; Tang, H.; Deng, H.; Zhou, X., Metal-organic frameworks for precise inclusion of single-stranded DNA and transfection in immune cells. *Nat. Commun.* **2018,** *9* (1), 1293.
36. Wang, S.; McGuirk, C. M.; Ross, M. B.; Wang, S.; Chen, P.; Xing, H.; Liu, Y.; Mirkin, C. A., General and Direct Method for Preparing Oligonucleotide-Functionalized Metal–Organic Framework Nanoparticles. *Journal of the American Chemical Society* **2017,** *139* (29), 9827-9830.
37. Jia, Y.; Wei, B.; Duan, R.; Zhang, Y.; Wang, B.; Hakeem, A.; Liu, N.; Ou, X.; Xu, S.; Chen, Z.; Lou, X.; Xia, F., Imparting biomolecules to a metal-organic framework material by controlled DNA tetrahedron encapsulation. *Scientific Reports* **2014,** *4*, 5929.
38. Wang, Z.; Fu, Y.; Kang, Z.; Liu, X.; Chen, N.; Wang, Q.; Tu, Y.; Wang, L.; Song, S.; Ling, D.; Song, H.; Kong, X.; Fan, C., Organelle-Specific Triggered Release of Immunostimulatory Oligonucleotides from Intrinsically Coordinated DNA–Metal–Organic Frameworks with Soluble Exoskeleton. *Journal of the American Chemical Society* **2017,** *139* (44), 15784-15791.
39. Taylor, K., Human Molecular Genetics. By T. Strachan and A. P. Read. Oxford: Bios Scientific Publishers. 1996. ISBN 1 872748 69 4. Pp. 596 + Index. £29.95. *Annals of Human Genetics* **2003,** *61* (3), 283-285.
40. Carthew, R. W.; Sontheimer, E. J., Origins and Mechanisms of miRNAs and siRNAs. *Cell* **2009,** *136* (4), 642-55.
41. Kroll, J.; Klinter, S.; Schneider, C.; Voß, I.; Steinbüchel, A., Plasmid addiction systems: perspectives and applications in biotechnology. *Microbial biotechnology* **2010,** *3* (6), 634-657.

42. Thomas, C. M.; Summers, D., Bacterial Plasmids. In *eLS*, John Wiley & Sons, Ltd: 2001.
43. Maurisse, R.; De Semir, D.; Emamekhoo, H.; Bedayat, B.; Abdolmohammadi, A.; Parsi, H.; Gruenert, D. C., Comparative transfection of DNA into primary and transformed mammalian cells from different lineages. *BMC Biotechnology* **2010,** *10* (1), 9.
44. Urban, J. H.; Vogel, J., A Green Fluorescent Protein (GFP)-Based Plasmid System to Study Post-Transcriptional Control of Gene Expression In Vivo. In *Riboswitches: Methods and Protocols*, Serganov, A., Ed. Humana Press: Totowa, NJ, 2009; pp 301-319.
45. Liang, K.; Ricco, R.; Doherty, C. M.; Styles, M. J.; Bell, S.; Kirby, N.; Mudie, S.; Haylock, D.; Hill, A. J.; Doonan, C. J.; Falcaro, P., Biomimetic mineralization of metal-organic frameworks as protective coatings for biomacromolecules. *Nat. Commun.* **2015,** *6*, 7240.
46. Krishan, A., Rapid flow cytofluorometric analysis of mammalian cell cycle by propidium iodide staining. *The Journal of Cell Biology* **1975,** *66* (1), 188.
47. Deitch, A. D.; Law, H.; deVere White, R., A stable propidium iodide staining procedure for flow cytometry. *Journal of Histochemistry & Cytochemistry* **1982,** *30* (9), 967-972.
48. Riccardi, C.; Nicoletti, I., Analysis of apoptosis by propidium iodide staining and flow cytometry. *Nature protocols* **2006,** *1* (3), 1458-61.
49. Pérez-Berná, A. J.; Rodríguez, M. J.; Chichón, F. J.; Friesland, M. F.; Sorrentino, A.; Carrascosa, J. L.; Pereiro, E.; Gastaminza, P., Structural Changes In Cells Imaged by Soft X-ray Cryo-Tomography During Hepatitis C Virus Infection. *ACS nano* **2016,** *10* (7), 6597-6611.
50. Conesa, J. J.; Otón, J.; Chiappi, M.; Carazo, J. M.; Pereiro, E.; Chichón, F. J.; Carrascosa, J. L., Intracellular nanoparticles mass quantification by near-edge absorption soft X-ray nanotomography. *Scientific Reports* **2016,** *6*, 22354.
51. Pederson, T., Molecular Biology of the Gene: by James D. Watson: W. A. Benjamin (1965): New York, New York. *FASEB journal : official publication of the Federation of American Societies for Experimental Biology* **2015,** *29* (11), 4399-401.
52. Chiappi, M.; Conesa, J. J.; Pereiro, E.; Sorzano, C. O. S.; Rodríguez, M. J.; Henzler, K.; Schneider, G.; Chichón, F. J.; Carrascosa, J. L., Cryo-soft X-ray tomography as a quantitative three-dimensional tool to model nanoparticle:cell interaction. *Journal of Nanobiotechnology* **2016,** *14* (1), 15.
53. Gentile, F.; Moretti, M.; Limongi, T.; Falqui, A.; Bertoni, G.; Scarpellini, A.; Santoriello, S.; Maragliano, L.; Proietti Zaccaria, R.; di Fabrizio, E., Direct imaging of DNA fibers: the visage of double helix. *Nano letters* **2012,** *12* (12), 6453-8.